JOURNAL OF SOLID STATE CHEMISTRY 100, 246–254 (1992)

The Fluorite-Related Anion-Excess Structure of $CeN_{0.222}O_{0.667}F_{1.333}$: Ordering of Defect Clusters

T. VOGT*

Institut Laue Langevin, B. P. 156X, 38042 Grenoble Cedex, France

AND E. SCHWEDA†

Institut für Anorganische Chemie, Universität Tübingen, Auf der Morgenstelle 18, D-74 Tübingen, Germany

Received February 18, 1992; accepted March 14, 1992

This investigation presents the preparation of $CeN_{0.222}O_{0.667}F_{1.333}$ by a solid-state reaction from a mixture of $CeN : CeF_3 : CeO_2 = 1 : 2 : 1.5$ and its structural investigation. The samples were annealed at 900°C in platinum tubes for different times. The basic structure found by powder neutron diffraction is anion-excess fluorite-related. The unit cell is an orthorhombic distortion of the cubic fluorite cell and has the space group *Abm*2. The lattice constants are $a = 577.71(2)$ pm, $b = 572.76(5)$ pm, and $c = 573.32(6)$ pm. The structure refined by Rietveld analysis shows that [1 : 0 : 2]- defect clusters are present. In samples prepared by longer annealing times an ordering of these clusters to larger aggregates, i.e., toward the vernier phases, was observed. This was deduced from full profile analysis without refining a structural model by comparing the instrumental resolution curves of several models.

Introduction

The flexibility of the fluorite structure toward anion excess and deficiency causes the large structural variety and complexity in fluorite-related structures. As defect elements, different clusters are formed containing octahedra (in case of the anion deficient) or cuboctahedra (in case of the anion excess) as center polyhedra. In both cases ordered clusters lead to superstructures in the fluorite lattice. Both octahedron and cuboctahedron are elements of a cubic closed packing (ccp) of anions. This shows that a defect is stabilized by a partial transformation of the primitive cubic anion lattice of the fluorite structure into a closer packed one.

Another possibility for a closer anion arrangement is realized in the vernier phases ($Mn X_{2n+1}$). Mackovicky and Hyde described them as "layer misfit structures" (*2, 6*). The transition to a closer anion packing is two-dimensional. Layers of 4^4- nets transform into 3^6- nets. Comparing a net of 3^6-layers to a net of 4^4-layers, it can be shown that the distance between layers is $2/\sqrt{3} = 1.155$ times bigger in the 4^4-net. This is shown in Fig. 1. Due to the different packing of atoms in the two nets, one can see that eight rows of 3^6-cells are almost commensu-

*Present address: Brookhaven National Laboratory Associated Universities, Inc. Upton, Long Island, NY 11973.

†To whom correspondence should be addressed.

0022-4596/92 $5.00

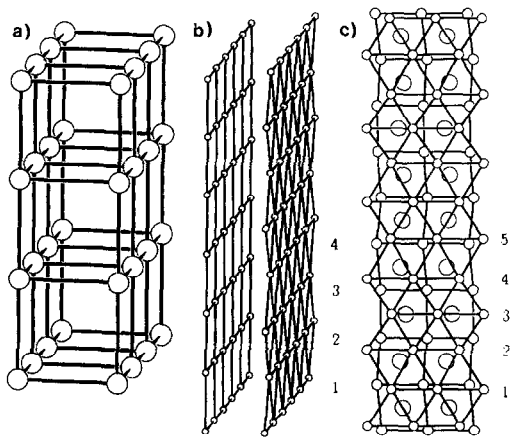

FIG. 1. Defects in the fluorite structure. (a) Anion cube in the fluorite structure. (b) Transformation of a 4^4-net in a 3^6-net in projection along the layers. (c) 3^6- and 4^4-net in projection onto the layers.

rate with seven rows of 4^4-cells. The exact geometrical ratio, to achieve commensurability of 3^6- to 4^4- cells, would be 8.08 : 7. If other ratios are realized in a structure, e.g., 6 : 5 in Dy_5Cl_{11} (*5*) or 5 : 4 in Eu_4Cl_9 (*4*), a modulation of the 3^6-layers and antiphase boundaries might occur on the unit cell level. In general one can distinguish between two types of vernier phases (*6*):

- with one cation-type.

Transformation of 4^4- to 3^6-nets takes place always in the same anion layer. This implies that no antiphase boundaries are present (see Fig. 5a).

- with different cation-types.

Modulated 3^6-layers are shifted by c/2 to form antiphase-boundaries (see 9)).

The reason why in the second case antiphase boundaries exist might be an ordering within the cation sublattice. An ordering of the anions by having the bigger anions with their higher charge (e.g., O^{2-}) in the less dense 4^4-net layers and the small and less charged anions (e.g., F^-) in the 3^6-net layers provides no reason for an antiphase boundary.

Bevan *et al.* showed that in the system $Y_nO_{n-1}F_{n+2}$ all members with even n crystallize in the space group *Pcmb* or it's subgroup $P112_1/b$, whereas those with odd n have the space group $Abm2$ (3). Mackovicky and Hyde defined a nomenclature for the vernier phases (*6*). The multiplicity p of a vernier phase is defined by the number m of 3^6-layers minus the number n of 4^4-layers:

$$m(3^6) - n(4^4) = p.$$

Using this nomenclature, $Zr_4ON_3F_5$ (*7*), for example, is a vernier phase with a multiplicity of one, since five 3^6-layers are commensurate with four 4^4-layers. It is said to form a "unit vernier phase." In the case of $Zr_{108}N_{98}F_{138}$ (*8*) we have 32 3^6-net layers matching 27 4^4-net layers. This leads to a multiplicity of five, i.e., a "multiple-vernier phase."

Before these types of "layer misfit structures" appear in a system one very often finds defect clusters, and it is only after longer annealing times of the samples that ordering takes place either by cation or anion diffusion. The statistical distributed defects in the structure can be interpreted as [1 : 0 : 4]-, [1 : 0 : 3]-, or [1 : 0 : 2]- clusters. See, for instance, Vogt *et al.* (*12*). We report here on ordered [1 : 0 : 2]-clusters, which can be seen as the intermediate state between statistically distributed defect clusters and ordered vernier phases.

Experimental

The preparation of anion-excess fluorite-related materials can be done by dopant cations of higher valency but same size (*9*) or by replacing, e.g., oxygen by fluorine atoms (*10, 11, 19, 20*). In the following we concentrate on samples with the formal stoichiometry $CeN_{0.222}O_{0.667}F_{1.333}$ prepared from a mixture of $CeN : CeF_3 : CeO_2 = 1 : 2 : 1.5$ but with different annealing times. We have a formal ratio of 2 : 1 for the relation of Ce^{3+} to Ce^{4+}. The first sample was annealed in

sealed platinum tubes at 950°C for 2 days (sample 1), the second sample for 2 weeks (sample 2). For elemental analysis the pyrohydrolysis method was used and N was determined: N = 1.2 (theor. = 1.7%) and F = 13.5% (theor. 14%).

Structural Investigations of $CeN_{0.222}O_{0.667}F_{1.333}$

The neutron powder diffraction experiments were done at the high-resolution diffractometer D2B (*18*) at the Institute Laue-Langevin in Grenoble, France. The obtained powder diffraction pattern could be indexed with an orthorhombic distorted fluorite cell. Pattern matching full profile refinements revealed that the space group was *Abm*2. This setting was choosen in order to compare directly with the results obtained by Bevan *et al.* in the system $Y_nO_{n-1}F_{n+2}$(*1, 3*).

In order to refine the structure it was assumed in a first model that the major part of the anion sublattice is made up of oxygen and fluorine. Since the scattering factors for oxygen (b = 5.805 fm) and fluorine (b = 5.654 fm) are quite similar, we used the one for oxygen throughout the refinement for all the anions. In the space group *Abm*2, anions were placed on the Wykoff positions 4*a*: 0,0,z, etc., and 4*b*: 1/2,0,*z*, etc. Ce was placed on 4*c*: *x*,1/4,*z*, etc. The model could be refined to an R_{wp} of 17.8% (R_{int} = 12.8%). This was a rather poor fit to the data. The misfit, especially in the low-angle region, revealed that some scattering density contributions were not taken into account by the model. With difference Fourier plots we were then able to locate scattering factor density on a general 8d position 0.153, 0.177, 0.408. Figure 3 shows this particular difference fourier plot parallel to the *ac*-plane in z = 0.18. Refining the model with this interstitial one obtains a satisfactory fit (shown in Fig. 2) and final reliability factors of R_{wp} = 9.5% and R_{int} = 4.6%. Table I gives the final parameters for $CeN_{0.22}O_{0.667}F_{1.333}$.

A similar good fit (R_{wp} = 9.5; R_I = 4.8) for the experimental data is obtained in space group *Pmmn* (see Table II) for a unit cell with the following relationship to the *Abm*2 cell: $a = a/\sqrt{2}$, $b = b/\sqrt{2}$, $c = c$. This corresponds to the space group for $SmF_{1.6}O_{0.7}$ as determined by Laval *et al.* (*17*). From powder data we cannot distinguish between the two alternative descriptions of the structure. However, as mentioned above we chose to use the *Abm*2 setting.

There are no indications in this sample for a possible superstructure. The resolution curve, which defines the full-width-half-maximum (FWHM) of the individual Bragg reflections, obtained from refining the machine parameters U, V, and W, is according to Caglioti's formulas (*14*):

$$(\mathrm{FWHM})^2 = U\tan^2\Theta + V\tan\Theta + W.$$

It shows that the normal instrumental resolution was reached with this sample, because no unusual, sample specific, peak broadening was observed (see Fig. 7, filled circles).

Discussion

The results of the structural refinement on $CeN_{0.222}O_{0.667}F_{1.333}$ can be interpreted by a model in which two interstitials are created for every vacancy. This is, in the notation of Willis, a [1 : 0 : 2]-cluster (*15*). The two facts, first, that no relaxed anion positions X''' were found in the structure, but only interstitials of the type X'', which in the cubic fluorite structure would correspond to positions (x,x,x), and second, the distortion of the cell from cubic to orthorhombic symmetry, point to an ordering of the defect clusters. If relaxed anion positions are possible or not seems to be related to the size of the cations and the charge of the anions. For example, in the case of $ThF_{0.76}O_{1.62}$ no

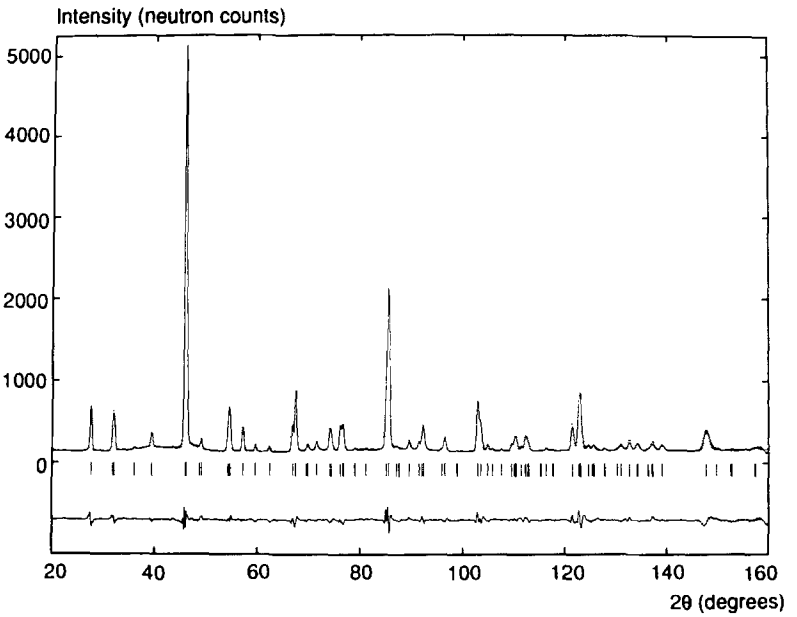

FIG. 2. Neutron diffraction diagram of a powder with composition $CeN_{0.222}O_{0.667}F_{1.333}$ (sample 1) and profile fit. Dotted lines = experimental intensities; full lines = calculated intensities. The tick marks indicate the Bragg reflections.

O^{2-} ions are found on relaxed anion positions (*16*).

Laval and Frit have shown that in the rare earth oxo-fluorides the size of the stable clusters depend on the size of the cations. In the case of the larger cations La^{3+}–Nd^{3+}, only [1 : 0 : 3]-clusters are found, whereas in the case of $SmF_{1.6}O_{0.7}$, [1 : 0 : 2]-clusters are present (*17*). In this system a very similar situation was found as in $CeN_{0.222}O_{0.667}F_{1.333}$. The structural investigation was done by X-ray powder diffraction and Rietveld refinement. This analysis revealed also partial ordering of [1 : 0 : 2]-clusters.

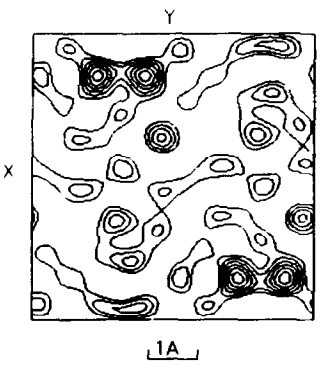

FIG. 3. Fourier section in $z = 0.18$, x parallel to [100], y parallel to [001], from 0 to 1.

The stoichiometrie $MX_{2.3}$ in $SmF_{1.6}O_{0.7}$ shows that the anion excess is too large to be adapted by ordering in a layered defect as in the vernier phases. The maximum in stoichiometry found so far for ordered vernier phases is $MX_{2.25}$ (M_4X_9). This can be explained by geometrical reasons (*4*). For the small rare earth cations Eu^{3+} to Lu^{3+}, ordered vernier phases exist. Therefore it was argued that ordered [1 : 0 : 2]-clusters are precursors for vernier phases. Figure 4 shows a comparison of the structure of a vernier phase with that of $CeN_{0.222}O_{0.667}F_{1.333}$. One notes that the anion

TABLE I

FINAL PARAMETERS FOR $CeN_{0.222}O_{0.667}F_{1.333}$ IN *Abm*2

Atom	*x*/*a*	*y*/*b*	*z*/*c*	*B*(Å^{-2})	Occupancy
Ce	0.7239(4)	0.25	0.324(2)	0.96(5)	1
O1	0.5	0.0	0.075	1.24(6)	1.01(1)
O2	0.0	0.0	0.093(1)	1.93(8)	0.86(1)
O3	0.153(1)	0.177(5)	0.408(5)	1.7(2)	0.16(1)

Note. R_{wp} = Weighted Profile *R*-value = $\frac{\sqrt{\Sigma[w(y_{obs} - y_{calc})^2]}}{\Sigma w(y_{obs})} \times 100\% = 9.5\%$.

R_I = Intensity Mod *I* *R*-value = $\frac{\Sigma[\text{mod}(I_{obs} - I_{calc}]}{\Sigma(I_{obs})} \times 100\% = 4.6\%$.

positions *X*(1) and *X*(2) in the 4^4-nets have different distances to the interstitials *X*(3). All possible 8*d* positions in *Abm*2 for the interstitial *X*(3) are drawn. Only 1/8 of them are occupied. This is symbolized by the full circles. In a phase M_4X_9 one interstitial per four fluorite subcells is accommodated in a 3^6-net layer. The fact that in $CeN_{0.222}O_{0.667}F_{1.333}$ only every eighth interstial site is occupied leads to a multiplicity between four and five for the corresponding vernier phase. The "vacancies" occur only in the *X*(2) layers. This is in agreement with the model, that [1 : 0 : 2]-clusters are precursors of the vernier phases, since only every second 4^4-net layer can be transformed into a 3^6-net layer. This and the fact that an orthorhombic distortion of the cubic fluorite cell is observed indicate that the defects are not distributed in an isotropic but rather in an anisotropic, thus ordered, way. The distances are comparable to those found in Ce_3NF_6 (see Table III). Figure 5 shows a [1 : 0 : 2]-cluster and indicates the relevant distances. We assume that the nitrogen is essentially in the *X*(1) positions and fluorine in the 8*d* positions *X*(3). The open questions of whether there is an ordering in the cation sublattice (Ce^{4+}, Ce^{3+}) and whether the transformation from the [1 : 0 : 2]-clusters to the vernier phase occurs with or without antiphase boundaries are still under investigation.

Defect Ordering

As already observed in the case of Ce_3NF_6, longer annealing times lead to an

TABLE II

FINAL PARAMETERS FOR $CeN_{0.222}O_{0.667}F_{1.333}$ IN *Pmmn*

Atom	*x*/*a*	*y*/*b*	*z*/*c*	*B*(Å^{-2})	Occupancy
Ce	0.25	0.25	0.2232(4)	1.07(3)	1
O1	0.75	0.25	0.075	1.14(3)	1
O2	0.75	0.25	0.498(1)	2.20(6)	0.84(1)
O3	0.25	0.095(2)	0.650(1)	1.6(2)	0.16(1)

Note. R_{wp} = Weighted Profile *R*-value = $\frac{\sqrt{\Sigma[w(y_{obs} - y_{calc})^2]}}{\Sigma w(y_{obs})} \times 100\% = 9.5\%$.

R_I = Intensity Mod *I* *R*-value = $\frac{\Sigma[\text{mod}(I_{obs} - I_{calc}]}{\Sigma(I_{obs})} \times 100\% = 4.8\%$.

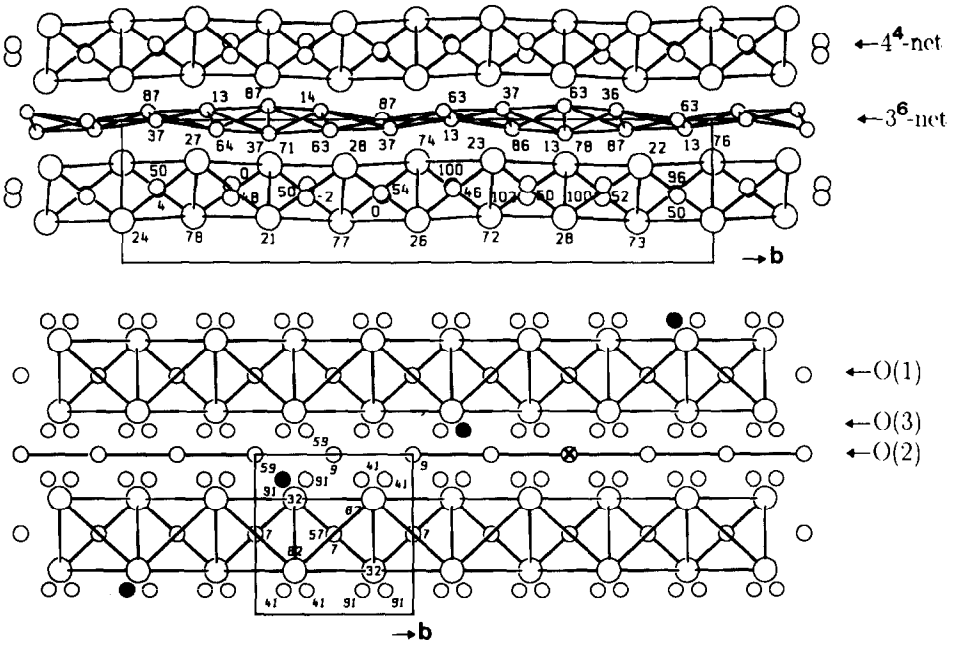

FIG. 4. Vernier-phase M_4X_9 (a) and [1 : 0 : 2]-Cluster (b) along [001]. Large circles = metal atoms, small circles = anions (O,N,F). Heights are in fractionate coordinates of $z \times 100$.

ordering of the defects. Figure 6 shows the neutron powder diffraction pattern of $CeN_{0.222}O_{0.667}F_{1.333}$, which was kept at 900°C for 2 weeks. The same model as for the less annealed sample was refined and proves to be inappropiate. Two important changes can be seen:

1. The appearance of small superlattice reflections around 40° in 2Θ.
2. The reflections at high 2Θ-values are too broad compared to the instrumental resolution function.

Attempts to refine a structural model of a vernier phase failed, but a full profile analysis provides evidence that the compound has at least partly ordered toward the structure of a vernier phase.

In a full profile analysis (often also called pattern matching) no structural model is needed to fit the data. Instead the intensities

TABLE III

BOND DISTANCES (Å) FOR $CeN_{0.222}O_{0.667}F_{1.333}$

Ce–O(1)	2.399(7)	Ce–O(3)″	2.59(3)	O(1)–O(3)″	2.94(2)
Ce–O(1)	2.408(7)	O(1)–O(1)	2.863(0)	O(2)–O(3)″	2.30(3)
Ce–O(2)	2.522(7)	O(1)–O(2)	2.8902(2)	O(2)–O(3)″	2.73(3)
Ce–O(2)	2.638(8)	O(1)–O(3)″	2.4(2)	O(2)–O(3)″	2.25(3)
Ce–O(3)″	2.55(1)	O(1)–O(3)″	2.89(2)	O(3)″–O(3)″	2.68(3)

Note. Standard deviations in paretheses; see Fig. 4. Dashes mark interstitials.

themselves are treated as parameters that are adjusted in a least-squares refinement. Refineable parameters are:

- the zeropoint correction for 2Θ,
- the cell constants determining the positions of the Bragg reflections in 2Θ,
- the socalled "machine parameters" $U,V,$ and W determining the full-width-half-maximum of the individual Bragg reflections
- and the individual intensities.

This method is more often used to deconvolute the individual intensities for ab inito structure determination using powder data, which then can be used in standard direct method approaches or Patterson techniques to determine the structure.

Point 1, above, indicates that a superstructure of some sort exists. Figure 4 shows that in our setting the ordering should occur along the b axis. By trying different multiple integers along b one notes that the first time any of the small superlattice reflections can be indexed is for the case of $n = 3$ (see Fig. 6). This agrees with the general classification mentioned above the vernier phases with odd n have the space group $Abm2$. If one continues to raise n beyond 5 the density of peaks becomes so large that no relevant conclusion can be drawn. However, if one

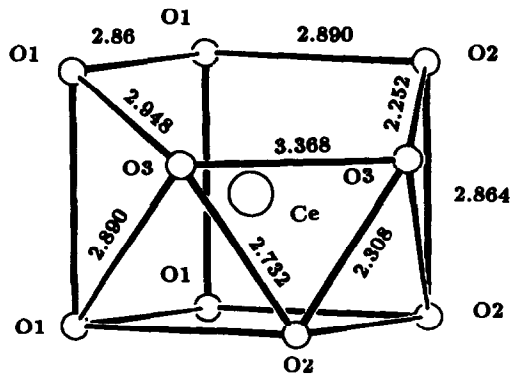

FIG. 5. Defect-cluster in $CeN_{0.22}O_{0.667}F_{1.333}$; distances within the polyhedron are in Å.

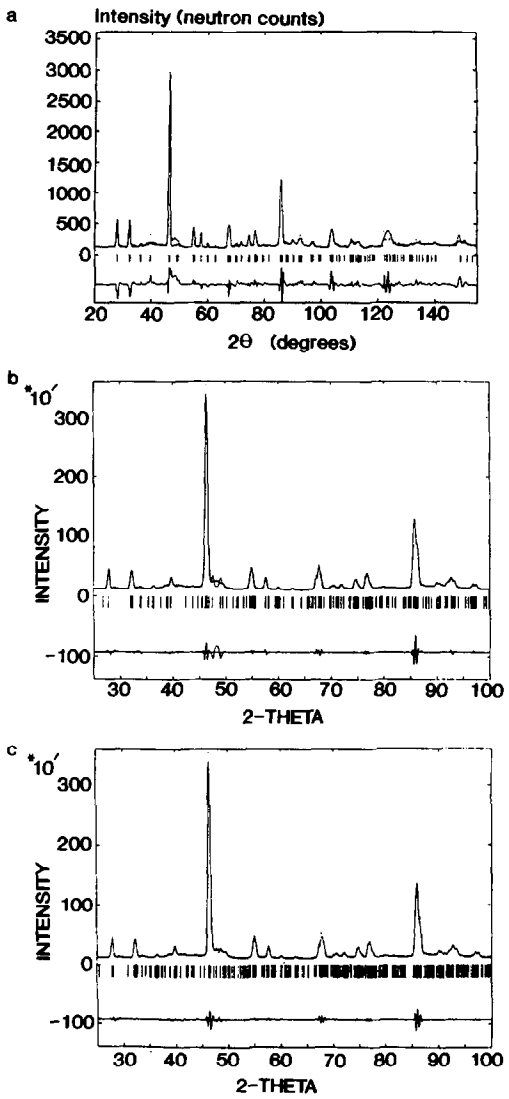

FIG. 6. Neutron diffraction diagram of sample 2, $CeN_{0.222}O_{0.667}F_{1.333}$, which was annealed for 2 weeks. (a) The Rietveld refinement using the same model as for sample 1 ($b = b_1$). (b) The full-profile-fitting for a cell with a, $3b_1$, c. Note that the little superlattice reflections can be indexed. (c) The full-profile-fit for a cell with a, $5b_1$, c.

analyzes the instrumental parameters one observes that for $n = 3$ (black dots) the resolution curve comes close to the one observed for the sample with the shorter an-

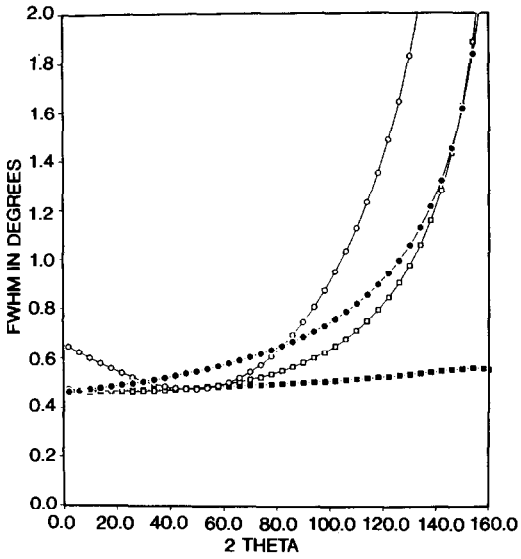

FIG. 7. Instrumental resolution curves for different models of $CeN_{0.222}O_{0.667}F_{1.333}$. The diagram shows the function $(FWHM)^2 = U\tan^2\Theta + V\tan\Theta + W$. (○) For sample 2 (see Fig. 6a) and $b = b_1$ the reflections are too broad. (■) For sample 2 (see Fig. 6c) and $b = 5b_1$ the reflections are too narrow compared to what is observed. (●) Sample 1 (see Fig. 2) and (□) sample 2 (see Fig. 6b) with $b = 3b_1$ follow the normal behavior.

nealing time (open squares in Fig. 7). For higher n the resolution curve then reveals a smaller FWHM of the Bragg reflections at high angles than the ones determined from standard samples. Thus n higher than five can be disregarded.

Conclusion

Full profile refinement can provide valuable insight into the "mesoscopic structure" of powders. Under a mesoscopic structure we understand, as pointed out by Salje (*21*), the nonhomogeneous structure of materials on a length scale of 100 Å and beyond, e.g., twin and domain structures, antiphase boundaries, stacking faults, and many more. Even though these microstructures have length scales larger than the interatomic distances, probed with standard diffraction methods, they often manifest themselves in powder pattern as deviations of certain groups of reflections from the resolution curve. Rodriguez-Carvajal has shown how microstrains of local orthorhombic distortions in an averaged tetragonal lattice lead to an anisotropic broadening of Bragg reflections (*22*). It is known that stacking faults reveal themselves by peak asymmetry and anisotropic broadening (*23*) of the resolution curve. Full profile fitting provides an easy way of detecting the presence of these "mesoscopic" features, since no structural model is assumed and thus a "best fit" will show any deviation from an "ideal" resolution curve. We attribute the deviations seen for $n = 3$ in Fig. 6 to these two effects. A complete analysis of this and other cases of stacking faults in vernier phases shall be given in another study. We can summarize that there is structural evidence from powder diffraction that the ordered [1 : 0 : 2]-cluster in $CeN_{0.222}O_{0.667}F_{1.333}$ transforms into a Vernier phase by long time annealing.

References

1. D. J. M. BEVAN AND A. W. MANN, *Acta Crystallogr. Sect. B* **31,** 1406 (1974).
2. B. G. HYDE, A. N. BAGSHAW, S. ANDERSSON, AND M. O'KEFFEE, *Annu. Rev. Mater. Sci.* **4,** 43 (1974).
3. D. J. M. BEVAN, J. MOHYLA, B. F. HOSKINS, AND R. J. STEEN, *Eur. J. Solid State Inorg. Chem.* **27,** 451 (1990).
4. R. BACHMANN, Thesis, Karlsruhe (1987).
5. C. RINCK, Thesis, Karlsruhe (1982).
6. F. MAKOVICKY AND B. G. HYDE, *Struct. Bonding* **46,** 101 (1981).
7. R. SCHLICHENMAIER, Thesis, Tübingen (1992).
8. W. JUNG AND R. JUZA, *Z. Anorg. Allg. Chem.* **399,** 129 (1973).
9. J. GALY AND R. S. ROTH, *J. Solid State Chem.* **7,** 277 (1973).
10. B. TANGUY, M. PEZAT, J. PORTIER, AND P. HAGENMULLER, *Mater. Res. Bull.* **6,** 57 (1971).
11. M. PEZAT, B. TANGUY, M. VLASSE, J. PORTIER, AND P. HAGENMULLER, *J. Solid State Chem.* **18,** 381 (1976).
12. T. VOGT, E. SCHWEDA, J. P. LAVAL, AND B. FRIT, *J. Solid State Chem.* **83,** 324 (1989).

13. H. M. RIETVELD, *J. Appl. Crystallogr.* **2,** 65 (1969).
14. G. CAGLIOTI, A. PAOLETTI, AND F. P. RICCI, *Nucl. Instrum. Methods* **3,** 223 (1958).
15. B. T. M. WILLIS *in* "The Chemistry of Extended Defects in Nonmetalic Solids" (L. Eyring and M. O'Keeffe, Eds.), Vol. 290, North-Holland, Amsterdam (1970).
16. J. P. LAVAL, A. ABAOUZ, B. FRIT, AND J. PANNETIER, *Eur. J. Solid State Inorg. Chem.* **26,** 23 (1989).
17. J. P. LAVAL, A. ABAOUZ, B. FRIT AND A. LE BAIL, *Eur. J. Solid State Inorg. Chem.* **27,** 545 (1990).
18. A. W. HEWAT AND I. BAILEY, *Nucl. Instrum. Methods* **137,** 463 (1976).
19. W. H. ZACHARIASEN, *Acta Crystallogr.* **4,** 231 (1951).
20. J. PANNETIER AND J. LUCAS, *C. R. Acad. Sci. Paris ser. C* **268,** 604 (1969).
21. E. SALJE, *Acta Crystallogr. Sect. A* **47,** 453 (1991).
22. J. RODRIGUEZ-CARVAJAL, *P. Phys. Condens. Matter* **3,** 3215 (1991).
23. M. M. J. TRACY, J. M. NEWSAM, M. W. DEEM, PROC. R. SOC. LONDON SER. A **433,** 499 (1991).